THE JOURNAL OF BIOLOGICAL CHEMISTRY VOL. 286, NO. 26, pp. 22777–22784, July 1, 2011

Inactivation Kinetics of a New Target of β-Lactam Antibiotics*[S]

Received for publication, March 15, 2011, and in revised form, April 13, 2011 Published, JBC Papers in Press, May 4, 2011, DOI 10.1074/jbc.M111.239988

Sébastien Triboulet[‡§¶], Michel Arthur[‡§¶], Jean-Luc Mainardi[‡§¶‖], Carole Veckerlé[‡§¶], Vincent Dubée[‡§¶], Angèle NGuekam-Moumi[‡§¶], Laurent Gutmann[‡§¶‖], Louis B. Rice[**], and Jean-Emmanuel Hugonnet[‡§¶1]

From the [‡]Centre de Recherche des Cordeliers, Laboratoire de Recherche Moléculaire sur les Antibiotiques, Equipe 12, Université Pierre et Marie Curie, Paris 6, UMR S 872, Paris, F-75006 France, the [§]Université Paris Descartes, UMR S 872, Paris, F-75006 France, [¶]INSERM, U872, Paris, F-75006 France, [‖]Assistance Publique-Hôpitaux de Paris, Hôpital Européen Georges Pompidou, Paris, F-75015 France, and [**]Rhode Island Hospital, Brown University, Providence, Rhode Island 02903-4923

Peptidoglycan is predominantly cross-linked by serine DD-transpeptidases in most bacterial species. The enzymes are the essential targets of β-lactam antibiotics. However, unrelated cysteine LD-transpeptidases have been recently recognized as a predominant mode of peptidoglycan cross-linking in *Mycobacterium tuberculosis* and as a bypass mechanism conferring resistance to all β-lactams, except carbapenems such as imipenem, in *Enterococcus faecium.* Investigation of the mechanism of inhibition of this new β-lactam target showed that acylation of the *E. faecium* enzyme (Ldt_{fm}) by imipenem is irreversible. Using fluorescence kinetics, an original approach was developed to independently determine the catalytic constants for imipenem binding ($k_1 = 0.061\ \mu M^{-1}\ min^{-1}$) and acylation ($k_{inact} = 4.5\ min^{-1}$). The binding step was limiting at the minimal drug concentration required for bacterial growth inhibition. The Michaelis complex was committed to acylation because its dissociation was negligible. The emergence of imipenem resistance involved substitutions in Ldt_{fm} that reduced the rate of formation of the non-covalent complex but only marginally affected the efficiency of the acylation step. The methods described in this study will facilitate development of new carbapenems active on extensively resistant *M. tuberculosis.*

β-Lactam antibiotics entered clinical trials in 1941 and have become and remained the most widely used family of drugs for the treatment of severe infections. The success of these molecules as therapeutic agents originates from a combination of properties, including low toxicity, excellent bioavailability, and broad-spectrum bactericidal activity. The latter property is accounted for by the conservation of the target, the active-site serine DD-transpeptidases, thought to catalyze an essential step in cell wall synthesis in all peptidoglycan-containing bacteria (1). The discovery of hundreds of β-lactams and of β-lactamase inhibitors has made it possible to partially compensate for the erosion of antibacterial activity due to the emergence of various mechanisms of resistance. In Gram-negative bacteria, these mechanisms mostly involve the production of β-lactamases, often associated with decreased outer membrane permeability and drug efflux. In Gram-positive bacteria, β-lactamase production is also frequent, but modification of the DD-transpeptidases is the clinically relevant mechanism in important pathogens, such as *Staphylococcus aureus*, *Streptococcus pneumoniae*, and the enterococci. More recently, bypass of the DD-transpeptidases by a novel class of peptidoglycan polymerases, the LD-transpeptidases, has been shown to convey high level resistance to all β-lactams, except the carbapenems, in mutants of *Enterococcus faecium* selected *in vitro* (2). Transpeptidases of the DD and LD specificities are structurally unrelated, contain different active-site nucleophiles (Ser *versus* Cys, respectively), and catalyze formation of different peptidoglycan cross-links (4⟶3 *versus* 3⟶3, respectively) (3). The two modes of peptidoglycan cross-linking involve two stem peptides carried by adjacent glycan chains that act as acyl donor and acceptor. The DD-transpeptidases cleave the D-Ala^4–D-Ala^5 bond at the extremity of a pentapeptide donor stem (hence the DD designation) and link the carbonyl of D-Ala^4 to the amine group located on the third residue of the acceptor (4⟶3 cross-links). The LD-transpeptidases use the same acceptor but act on a different peptide bond of the donor stem, which consists of a tetrapeptide in most bacterial species. Transpeptidation proceeds through cleavage of the bond between the L center of the amino acid at the third position and D-Ala^4 (LD specificity) prior to formation of 3⟶3 cross-links. β-Lactam antibiotics act as a suicide substrate of the DD-transpeptidases because the active-site Ser residue attacks the carbonyl of the β-lactam ring (1). Because the resulting ester bond is hydrolyzed at a very slow rate, typically 2–10 h^{-1}, formation of the acylenzyme is considered to lead to irreversible inactivation of the enzyme at a physiologically relevant time scale. The active-site Cys residues of LD-transpeptidases similarly form thioester bonds with the β-lactam ring (4) (Fig. 1). The enzymes display narrow substrate specificity because this reaction occurs only with β-lactams of the carbapenem class.

In most bacteria, formation of 3⟶3 cross-links by LD-transpeptidases has a marginal role in peptidoglycan synthesis (2). For example, ~5 and 10% of the cross-links are of the 3⟶3 type during the exponential and stationary phases of growth in *Escherichia coli*, respectively. Genetic evidence has been provided

* This work was supported, in whole or in part, by National Institutes of Health, NIAID, Grants RO1 AI45626 and AI046626. This work was also supported by the Fondation pour la Recherche Médicale (Equipe FRM 2006; DEQ200661107918).

[S] The on-line version of this article (available at http://www.jbc.org) contains supplemental "Experimental Procedures" and supplemental Figs. S1–S5.

[1] Recipient of FRM Fellowship FDT 20080914133. To whom correspondence should be addressed: Centre de Recherche des Cordeliers, UMRS-872-Equipe 12, 15 Rue de l'Ecole de Médecine, 75006 Paris. E-mail: jean-emmanuel.hugonnet@crc.jussieu.fr.

for the inessential role of this mode of transpeptidation in *E. coli*. In wild type strains of *E. faecium*, LD-transpeptidation also has a marginal role in peptidoglycan transpeptidation (3% of 3→3 cross-links). However, serial selection for resistance to ampicillin, a β-lactam of the penicillin class, resulted in a mutant, M512, that exclusively relied on LD-transpeptidation in medium containing the drug (5). The capacity of the LD-transpeptidase of *E. faecium* (Ldt$_{fm}$) to bypass the DD-transpeptidases led to high level resistance to all β-lactams, except the carbapenems, that inactivate the enzyme, as stated above. *Mycobacterium tuberculosis* is the only known bacterium that displays a high (80%) content of 3→3 cross-links (6). Carbapenems were recently recognized as promising agents in the treatment of tuberculosis because these drugs are bactericidal against extensively drug-resistant (XDR) strains of *M. tuberculosis* (7). Carbapenems were active in association with clavulanic acid, a β-lactamase inhibitor that irreversibly inactivates the broad-spectrum BlaC β-lactamase constitutively produced by members of this species (8). Because carbapenems inactivate the LD-transpeptidases of *M. tuberculosis*, one of which is essential for virulence in a mouse model of acute infection (6, 9), LD-transpeptidases are likely to be the targets of carbapenems in *M. tuberculosis*.

An understanding of the mechanisms of resistance to antibiotics is critical to accurately detect resistant bacteria in clinical settings, to anticipate and prevent emergence of novel resistance phenotypes, and to design new drugs active against resistant bacteria. The mechanisms of acquisition of β-lactam resistance by modification of the classical DD-transpeptidases have been extensively studied (1). In contrast, nothing is known about the mechanism of acquisition of carbapenem resistance by modification of LD-transpeptidases despite the high potential of this class of drug in the treatment of tuberculosis. For this reason, we have investigated emergence of carbapenem resistance in *E. faecium* M512, a model bacterium that has the capacity to manufacture a peptidoglycan exclusively cross-linked by a single LD-transpeptidase (Ldt$_{fm}$) (4). This mutant is highly resistant to ampicillin, with a minimal inhibitory concentration (MIC)[2] higher than 2,000 μg/ml, but remains susceptible to the carbapenem imipenem (MIC = 0.5 μg/ml). We report the emergence of LD-transpeptidase-mediated carbapenem resistance, the identification of the corresponding substitutions in the target, and the development of spectroscopic methods that allowed us to understand the consequences for these modifications on the efficiency of enzyme acylation. These analyses provide, for the first time, evidence for a direct correlation between the catalytic constants of the target and the antibacterial activity of the drug.

EXPERIMENTAL PROCEDURES

Chemicals

Imipenem was a gift from Merck. Hydrolyzed imipenem was obtained by sodium hydroxide treatment (0.1 N), followed by neutralization with HCl. All buffers were purchased from Sigma. Ampicillin was obtained from Bristol-Myers-Squibb (Paris, France).

[2] The abbreviation used is: MIC, minimal inhibitory concentration.

Bacterial Strains and Selection of Mutants Resistant to Imipenem

All cultures were performed at 37 °C in brain heart infusion agar or broth. Spontaneous mutants S1–S4 were obtained from *E. faecium* M512 (5) by four serial selection steps on agar containing increasing concentrations of imipenem (2, 4, 8, and 16 μg/ml). Mutants S5–S11 were obtained from mutant S4 in seven selection steps in broth containing 4 μg/ml imipenem and increasing concentrations of ampicillin (16, 64, 128, 256, 512, 1,000, and 8,000 μg/ml). MICs of ampicillin, of imipenem, and of ampicillin in the presence of a fixed concentration of imipenem were determined by the agar dilution method after 48 h of incubation.

Purification of LD-Transpeptidases

We have previously described the construction of a derivative of vector pET2818 encoding domains I and II of Ldt$_{fm}$ (residues 119–466) fused to a C-terminal 6-histidine tag (GSH_6)(3). Derivatives of pET2818 containing the same portion of the *ldt$_{fm}$* gene with mutations leading to G430S, S405N, or both amino acid substitutions were constructed as described in the supplemental "Experimental Procedures". Wild-type and mutant Ldt$_{fm}$ were produced in *E. coli* BL21 and purified by metal affinity and size exclusion chromatographies (supplemental "Experimental Procedures"). Protein concentration was determined by the Bradford method (Bio-Rad protein assay).

Kinetic Analyses

Spectrophotometry—Formation of the acylenzyme (*EI**) in 100 mM sodium-phosphate (pH 6.0) was determined at 10 °C by measuring the decrease in absorbance at 299 nm resulting from opening of the β-lactam ring of imipenem. The difference ($\Delta\epsilon_{299\ nm} = -7{,}100\ M^{-1}\ cm^{-1}$) was deduced from the molar extinction coefficient of imipenem ($7{,}700\ M^{-1}\ cm^{-1}$) and of hydrolyzed imipenem ($600\ M^{-1}\ cm^{-1}$). Fast kinetics were performed with a stopped-flow apparatus RX-2000 (Applied Photophysics) coupled to a Cary 100-Bio spectrophotometer (Varian SA).

Spectrofluorimetry—All fluorescence measurements were performed with a stopped-flow apparatus RX-2000 coupled to a Cary Eclipse spectrofluorimeter (Varian SA) in 100 mM sodium phosphate (pH 6.0) at 10 °C. The Trp residues were excited at 225 nm with a slit of 5 nm and an optical path length of 2 mm. Fluorescence emission was determined at 335 nm with a slit of 5 nm and an optical path length of 10 mm. The detector voltage was set to 600 V.

Inactivation Kinetics Simulation—According to reaction scheme II (Fig. 1), the variations in the concentrations of the three forms of the enzyme over time can be defined for free enzyme ($d[E]/dt = k_{-1}[EI] - k_1[E][I]$, which is equal to $d[I]/dt$), for the non-covalent complex ($d[EI]/dt = k_1[E][I] - k_{inact}[EI]$), and for the acylenzyme ($d[EI^*]/dt = k_{inact}[EI]$). Using the initial conditions ($[E] = [E_{total}]$ and $[I] = [I_{total}]$ at time = 0), the concentrations of the three forms of the enzyme were iteratively computed for sequential time increments of 0.005 min using Excel software (Microsoft). Fluorescence intensity (*F*) was calculated using the relative fluorescence intensities of the three forms of the enzyme ($F = a[E] + b[EI] + c[EI^*]$). In cer-

tain simulations, the fluorescence intensity was normalized ($F_{norm} = F/a[E_{total}]$) in order to simplify comparisons of kinetics obtained with different concentrations of imipenem. In order to fit simulations with experimental data, we generated four parallel plots with four different concentrations of imipenem. The catalytic constants (k_1, k_{-1}, and k_{inact}) and the relative fluorescence intensity of *E*I were adjusted to simultaneously obtain the best superposition between the simulations and the experimental data in the four plots.

RESULTS

Irreversible Inactivation of Wild-type Ldt$_{fm}$ by Imipenem—Based on the mechanism of Ldt$_{fm}$ inactivation by imipenem (Fig. 1), we initially considered three steps (Fig. 1, *Scheme 1*), including (i) formation of a non-covalent complex (*E*I) comprising enzyme and inhibitor, (ii) formation of the acylenzyme (*E*I*), and (iii) hydrolysis of *E*I* that would generate native enzyme and hydrolyzed inhibitor. To determine whether Ldt$_{fm}$ participates in this full catalytic cycle, various concentrations of Ldt$_{fm}$ (5, 10, 15, and 20 μM) were incubated with an excess of imipenem (100 μM), and rupture of the β-lactam ring was determined by measuring the absorbance at 299 nm (supplemental Fig. S1). The kinetics showed a rapid decrease in absorbance (Fig. 2*A*), the amplitude of which was commensurate with rupture of 1 molar equivalent of β-lactam ring/mol of enzyme (Fig. 2*B*). Thus, Ldt$_{fm}$ was fully acylated by imipenem under these conditions. The absence of any further decrease in absorbance shows that the enzyme did not detectably turn over because this would result in the rupture of β-lactam rings in stoichiometric excess to enzyme. Thus, inactivation of Ldt$_{fm}$ was irreversible at this time scale. In order to determine whether enzyme turnover could be detected at a larger time scale, imipenem (100 μM) was incubated with enzyme (2.5 μM) for 1,000 min at room temperature (Fig. 2*C*). Control kinetics indicated that spontaneous hydrolysis of imipenem occurred slowly with an apparent pseudo-first-order rate of 5×10^{-4} min^{-1}. The rate of decrease in absorbance was not modified by the presence of Ldt$_{fm}$, indicating that hydrolysis of imipenem due to enzyme turnover, if any, is even lower ($\leq 1 \times 10^{-4}$ min^{-1}). This upper limit corresponds to <1 catalytic cycle/day. The stability of the acylenzyme was also assessed by mass spectrometry. For this approach, *E*I* was prepared by incubating enzyme (100 μM) with imipenem (200 μM). Excess imipenem was removed by size exclusion chromatography, and the purified acylenzyme was incubated for 1,000 min at room temperature and analyzed by mass spectrometry, as described previously (4). Under such conditions, no formation of native enzyme, imipenem, or hydrolyzed imipenem from the acylenzyme was detected. Thus, formation of the acylenzyme was irreversible, and reaction scheme 2 (Fig. 1, *Scheme 2*) was used for further analyses of the inactivation reaction.

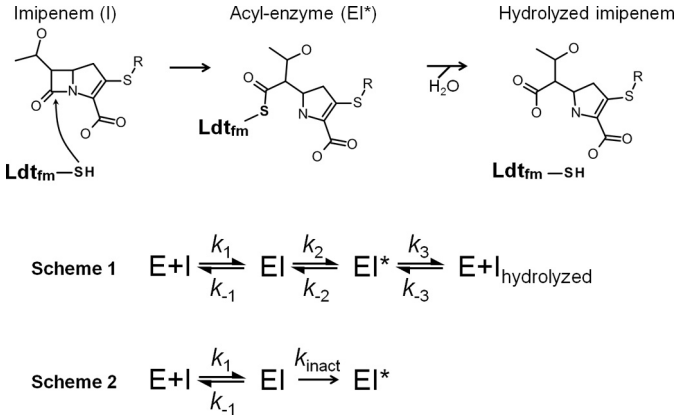

FIGURE 1. **Acylation of Ldt$_{fm}$ by imipenem.** Imipenem is a suicide substrate of the LD-transpeptidase. Nucleophilic attack of the carbonyl of the β-lactam ring by the sulfur of the catalytic cysteine results in the formation of a thioester bond. The resulting acylenzyme is potentially hydrolyzed, thereby generating free enzyme and hydrolyzed imipenem. Reaction scheme 1 (*Scheme 1*) describes a full catalytic cycle comprising three reversible steps. Reaction scheme 2 (*Scheme 2*) describes irreversible enzyme acylation.

Determination of Catalytic Constant k_{inact} by Spectrophotometry—The kinetics of Ldt$_{fm}$ acylation were determined by measuring the reduction in absorbance due to the rupture of the β-lactam ring. Kinetics were determined for seven concentrations of imipenem at 10 °C to slow down the reaction. Regression was performed for each time course, and the first order constant (k_{obs}) was plotted as a function of the concentration of imipenem (Fig. 3). Regression analysis of the two-step reaction provided values of 4.5 ± 0.6 min^{-1} for k_{inact} and 41 ± 2 μM for K_{app}. The constant k_{inact} represents the maximum rate of the inactivation reaction for saturating concentrations of imipenem. The constant K_{app} is analogous to the classical Michaelis constant, K_m, which can be equated to the dissociation constant K_D (k_{-1}/k_1) only if *E*, I, and *E*I are in rapid equilibrium (k_{-1} and k_1[I] are both much larger than k_{inact}). As shown below, this condition does not apply to inactivation of wild-type Ldt$_{fm}$ by imipenem.

Determination of the Catalytic Constant k_1 by Spectrofluorimetry—The intrinsic fluorescence of Ldt$_{fm}$ was determined by exciting Trp residues at 225 nm and measuring emission at 335 nm (supplemental Fig. S2). Imipenem and hydrolyzed imipenem were not fluorescent at these wavelengths. The fluorescence time course was biphasic (Fig. 4*A*). In the first phase, the fluorescence

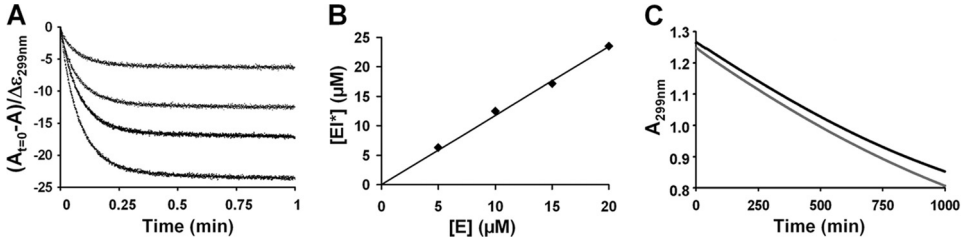

FIGURE 2. **Irreversible acylation of Ldt$_{fm}$ by imipenem.** *A*, kinetics of acylation of Ldt$_{fm}$ (5, 10, 15, and 20 μM) by imipenem (100 μM) were followed by absorbance at 299 nm. In order to estimate the concentration of imipenem with a ruptured β-lactam ring, the reduction in absorbance ($A_t = A_0 - A$) was divided by the difference in the molar extinction coefficients of imipenem and hydrolyzed imipenem $\times 10^{-6}$ ($\Delta\epsilon = -7{,}100$ M^{-1} cm^{-1}). *B*, the concentration of imipenem with a ruptured β-lactam ring was plotted as a function of enzyme concentration. *C*, imipenem (100 μM) was incubated in the absence (*lower gray curve*) or in the presence (*upper black curve*) of Ldt$_{fm}$ (2.5 μM).

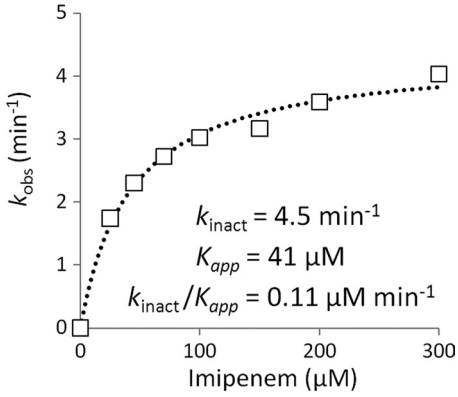

FIGURE 3. **Kinetic analyses of Ldt$_{fm}$ inactivation by spectrophotometry.** Ldt$_{fm}$ (10 μM) was incubated with imipenem (25, 45, 70, 100, 150, 200, and 300 μM), and regression analyses of the kinetics of formation of the acylenzyme (*EI**) were performed with the equation, $[EI^*] = [E_{total}](1 - e^{-k_{obs}t})$, in which $[E_{total}]$ represents the total enzyme concentration, k_{obs} is a constant, and t is time. For determination of the catalytic constants k_{inact} and K_{app}, the values of k_{obs} were plotted as a function of imipenem concentration [I], and regression analysis was performed using the equation, $k_{obs} = k_{inact}[I]/K_{app} + [I]$, in which k_{inact} is the first-order constant for acylenzyme formation, and K_{app} is a constant.

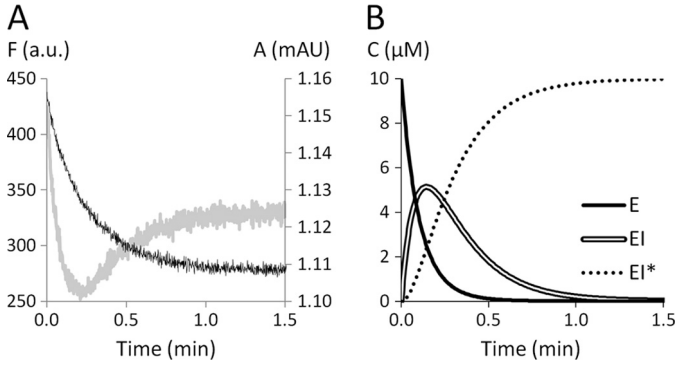

FIGURE 4. **Detection of the non-covalent complex by spectrofluorimetry.** *A*, Ldt$_{fm}$ (10 μM) was incubated with imipenem (150 μM), and enzyme inactivation was monitored by spectrofluorimetry (*gray curve*). Fluorescence intensity (arbitrary units (*a.u.*); *left axis*) was determined at λ_{ex} = 225 nm and λ_{em} = 335 nm. Absorbance (milliabsorbance units (*mAU*); *right axis*) was determined at 299 nm (*black curve*). *B*, simulation of the variations in the concentrations of the three forms of the enzyme. The initial concentrations of enzyme ($E = E_{total}$ at time 0) and inhibitor ($I = I_{total}$ at time 0) were 10 and 150 μM, respectively. The values 0.065 μM^{-1} min^{-1}, 0.1 min^{-1}, and 4.5 min^{-1} were attributed to the catalytic constants k_1, k_{-1}, and k_{inact}, respectively.

intensity decreased rapidly to reach a minimum. In the second phase, the fluorescence intensity increased more slowly and reached a steady state value intermediary between the initial value and the minimum. Because the first phase was more rapid than formation of the acylenzyme detected by spectrophotometry (Fig. 4*A*), the initial decrease in fluorescence was due to formation of a reaction intermediate that should correspond to the non-covalent complex *E*I, according to scheme 2 (Fig. 1). Qualitatively, this implies that the fluorescence of *E* is greater (22%) than that of *EI** because these two forms of the enzyme are exclusively present at the beginning of the reaction ($t = 0$) and after complete enzyme acylation, respectively. This also implies that intense fluorescence quenching upon formation of *E*I is responsible for the initial decrease in fluorescence.

In order to simulate fluorescence kinetics, we computed the variations in the concentrations of *E*, *E*I, and *EI** according to catalytic constants k_1, k_{-1}, and k_{inact} defined in scheme 2 of Fig. 1 (see "Experimental Procedures"). As shown in the simulation depicted in Fig. 4*B*, free enzyme rapidly disappears in the first phase of the reaction mainly due to formation of the non-covalent complex. This accounts for the initial decrease in fluorescence intensity, which reaches a minimum when accumulation of *E*I is at its maximum. In the second phase of the reaction, *EI** accumulates at the expense of *E*I, leading to an increase in fluorescence intensity until a plateau is reached after complete enzyme acylation. Simulations of fluorescence kinetics were performed by attributing relative fluorescence intensities to the three forms of the enzyme and computing the sum of the contributions of these three forms. Examples of these simulations appear as *dotted lines* in Fig. 5.

In order to determine the catalytic constants of Ldt$_{fm}$, the fluorescence kinetics obtained with four concentrations of imipenem were fitted to simulations constructed with different values for the catalytic constants k_1 and k_{-1} and for the relative fluorescence of *E*I (Fig. 5). Other parameters were independently determined, including k_{inact} (see above; Fig. 3) and the relative fluorescence intensities of free enzyme (*E*) and of the acylenzyme (*EI**), which were obtained with purified forms of the enzyme (supplemental Fig. S2). A single combination of values for k_1 and the fluorescence intensity of *E*I allowed us to fit the experimental data to the simulations (Fig. 5). Constant k_{-1} could be set to zero or to any arbitrary value smaller than 0.1 min^{-1}. The value of k_1 deduced from this analysis, 0.065 μM^{-1} min^{-1}, indicates that the pseudo-first-order constant k_1[I] is in the order of magnitude of k_{inact} if the concentration of imipenem is equal to 100 μM (6.5 *versus* 4.5 min^{-1}, respectively). Thus, formation of the non-covalent complex and enzyme acylation were both limiting under our assay conditions. The low value of k_{-1} (<0.1 min^{-1}) in comparison with k_{inact} (4.5 min^{-1}) indicates that dissociation of *E*I is negligible. Thus, the complex is committed to acylation.

The properties of Ldt$_{fm}$ indicate that a decrease in the efficiency of enzyme acylation could potentially originate from mutational alterations, leading to decreases in the values of k_1, k_{inact}, or both catalytic constants, an increase in k_{-1}, or exposure of the acylenzyme to hydrolysis. In order to determine which of these mechanisms could be relevant to the emergence of imipenem resistance, our next objective was to select mutants of *E. faecium* resistant to this drug.

Emergence of Resistance to Imipenem—We have previously reported activation of the LD-transpeptidation pathway under the selective pressure of ampicillin in *E. faecium* (5). Selection by this drug led to mutant M512, which is highly resistant to all β-lactams except carbapenems (Fig. 6) because Ldt$_{fm}$ is selectively inactivated by the drugs. In order to determine whether *E. faecium* can gain imipenem resistance by further modifications of the LD-transpeptidation pathway, we selected mutants of M512 by serial subcultures on medium containing increasing concentrations of this drug. Mutant S4, obtained in four steps, displayed a 32-fold increase in the MIC of imipenem (Fig. 6). However, this mutant was unable to grow in the presence of both ampicillin and imipenem. This indicates that the DD-transpeptidases retained an essential contribution to peptidoglycan cross-linking because ampicillin inactivates these enzymes but not Ldt$_{fm}$ (4). The selection procedure was therefore continued

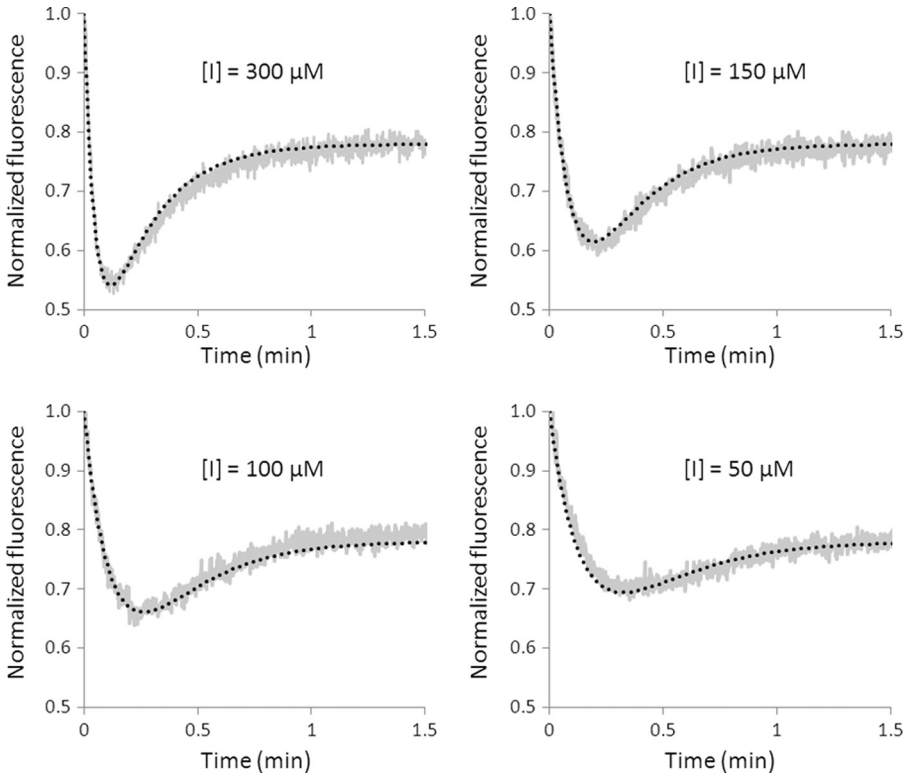

FIGURE 5. **Analyses of Ldt$_{fm}$ inactivation at various concentrations of imipenem by spectrofluorimetry.** Ldt$_{fm}$ (10 μM) was incubated with imipenem (300, 150, 100, and 50 μM), and enzyme inactivation was monitored by spectrofluorimetry. The *gray* and *dotted black curves* correspond to normalized fluorescence for experimental data points and a simulation, respectively. The simulation was performed with values of 0.065 μM^{-1} min^{-1}, 0.1 min^{-1}, and 4.5 min^{-1} for the catalytic constants k_1, k_{-1}, and k_{inact}, respectively. The relative fluorescence intensities used for the simulation were 750, 250, and 585 arbitrary units for *E*, *EI*, and *EI**, respectively.

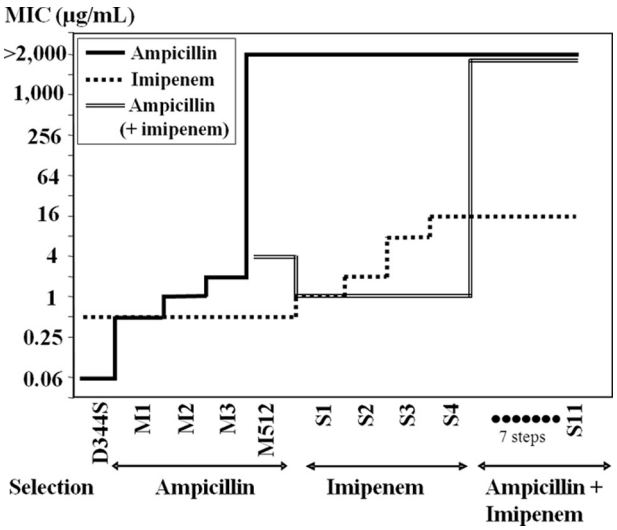

FIGURE 6. **MICs of β-lactams for *E. faecium* mutants.** Mutants M1, M2, M3, and M512 were obtained by four consecutive selections steps on increasing concentrations of ampicillin. Four additional selection steps with imipenem led to mutant S4, which was resistant to imipenem (MIC = 16 μg/ml) but remained susceptible to ampicillin (4 μg/ml) in the presence of imipenem (2 μg/ml). MICs of ampicillin were determined in the presence of 0.5, 1, and 2 μg/ml imipenem for mutants S1, S2, and S3. Mutant S11 was obtained from mutant S4 by seven selection steps in broth containing 4 μg/ml of imipenem and increasing concentrations of ampicillin. This mutant was resistant to the combination of imipenem (4 μg/ml) and ampicillin (>2,000 μg/ml).

by selecting for increasing resistance to ampicillin in the presence of imipenem at 4 μg/ml, a concentration that inhibited the parental strain M512 but not S4. Seven selection steps with this drug combination led to mutant S11, which grew in the presence of both ampicillin and imipenem.

Identification of Amino Acid Substitutions in Ldt$_{fm}$—Sequencing the *ldt$_{fm}$* gene of mutant S11 revealed two point mutations that led to amino acid substitutions S405N and G430S, both located in the catalytic domain of the LD-transpeptidase (supplemental Fig. S3). Sequencing of *ldt$_{fm}$* from the intermediary mutants showed that the two mutations appeared sequentially at the eighth (S405N) and 11th (G430S) selection steps. Substitution S405N is located at the entrance of the catalytic cavity in the loop connecting sheets β13 to β14. This loop forms a bridge on the top of the cavity, thereby defining the two access paths to catalytic Cys^{442} (10). Substitution G430S, which is more distant from Cys^{442}, affects the loop connecting helix α4 to sheet β15.

Kinetics of Inactivation of LD-Transpeptidases from Mutants Resistant to Imipenem—In order to analyze the impact of substitutions G430S and S405N on the catalytic constants, we constructed and purified derivatives of Ldt$_{fm}$ harboring these two substitutions alone or in combination. The absorbance and fluorescence spectra of the native and acylated enzymes remained similar to those of the wild-type enzyme (supplemental Fig. S2). The value of k_{inact} was determined by spectrophotometry (Fig. 7*A*) and used to obtain k_1 by simulation of fluorescence kinetics (Fig. 7*B*), as described above for the wild-type enzyme. Substitution G430S produced a minor decrease in k_{inact} (from 4.5 to 3.2 min^{-1}), whereas k_1 was decreased ~16-fold (from 0.065 to 0.0040 μM^{-1} min^{-1}). Increasing the concentration of imi-

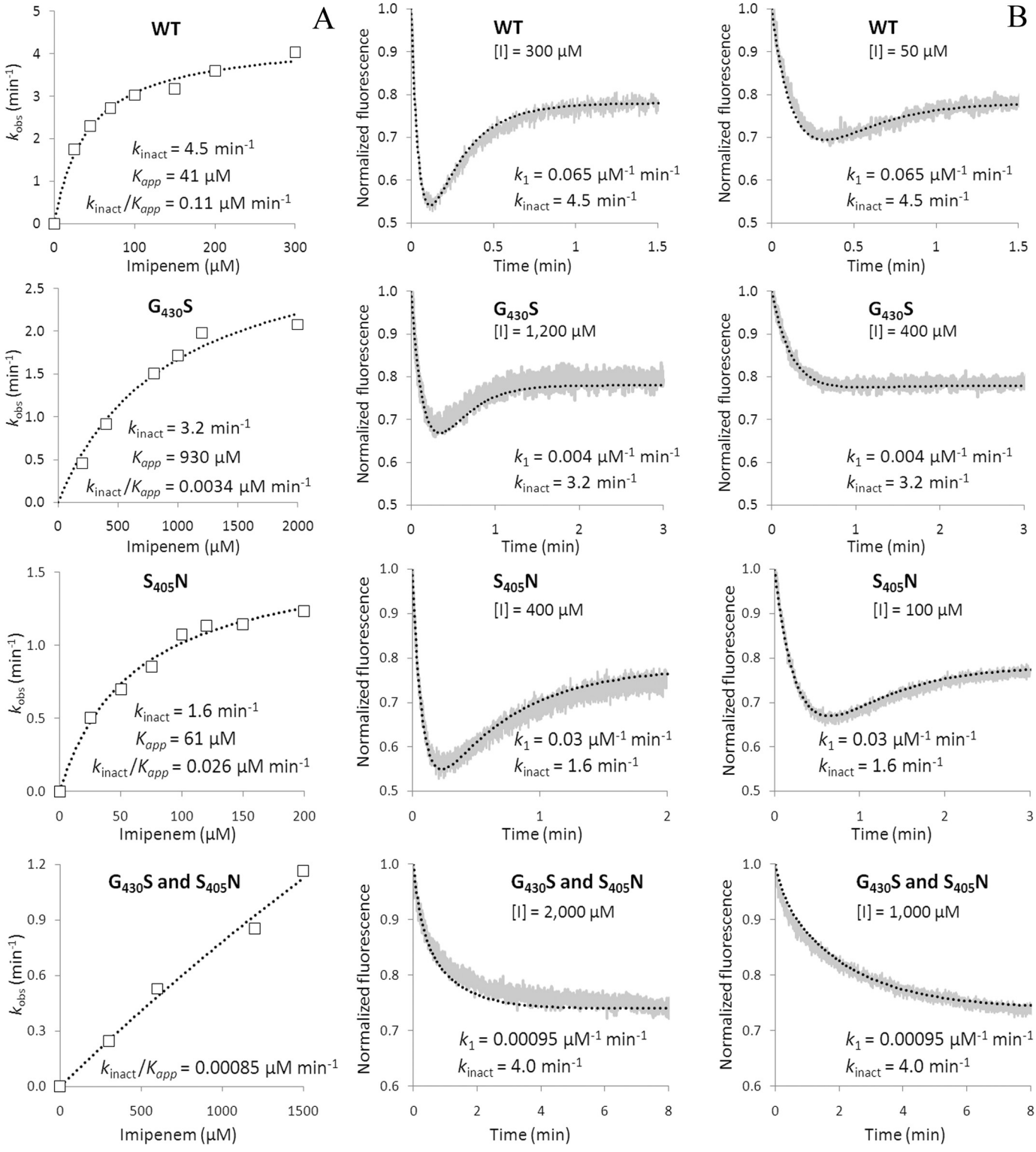

FIGURE 7. **Impact of amino acid substitutions S405N and G430S on the kinetics of Ldt$_{fm}$ inactivation by imipenem.** *A*, determination of the catalytic constants k_{inact} and K_{app} by spectrophotometry. The values of k_{obs} were plotted as a function of imipenem concentration [I], and regression analysis was performed using the equation, $k_{obs} = k_{inact}[I]/K_{app} + [I]$, in which k_{inact} is the first-order constant for acylenzyme formation and K_{app} is a constant. *B*, determination of the catalytic constants k_1 by spectrofluorimetry. The charts present examples of kinetics at two different concentrations of imipenem. The *gray* and *black curves* correspond to normalized fluorescence for experimental data points and the simulations, respectively. The simulations were performed with the indicated values of k_1 and k_{inact}. A value of 0.1 min^{-1} was used for k_{-1} for all kinetics. *WT*, wild-type enzyme.

penem led to fluorescence kinetics similar to those of the wild-type enzyme, indicating that the decrease in k_1 could be compensated by an increase in the concentration of imipenem, as expected from reaction scheme 2 (Fig. 1). The second substitution, S405N alone, caused moderate decreases in k_{inact} (from 4.5 to 1.6 min^{-1}) and k_1 (from 0.065 to 0.030 μM^{-1} min^{-1}). Com-

bination of the two substitutions led to an enzyme that retains a k_{inact} value similar to that of the wild-type enzyme (4.0 *versus* 4.5 min^{-1}) but displayed a 68-fold reduction in k_1 (from 0.065 to 0.00095 μM^{-1} min^{-1}). Together these results indicate that the emergence of imipenem resistance was not associated with any major decrease in the efficiency of the chemical step of the acylation reaction. Rather, the two amino acid substitutions, which were serially selected by imipenem, resulted in a dramatic decrease in k_1. As stated above, both the formation of the *E*I complex and the acylation step are limiting for the wild-type enzyme. This situation also prevailed in the mutants, and the simulation of fluorescence kinetics indicated that the value of k_{-1} remained low in comparison with k_{inact}. Thus, mutant S11 escaped inhibition by low concentrations of imipenem mainly because its LD-transpeptidase formed a non-covalent complex with the drug at a lower rate than the wild-type enzyme.

DISCUSSION

Clinically relevant mechanisms of β-lactam resistance in *S. aureus*, *S. pneumoniae*, and *E. faecium* involve production of "low affinity" penicillin-binding proteins. The "low affinity" designation is imprecise because inefficient inactivation of these DD-transpeptidases by β-lactams often results from low acylation rates in addition to low affinities for the drugs (11). Bypass of the classical DD-transpeptidases by an LD-transpeptidase, as originally detected in an *in vitro*-selected *E. faecium* mutant, M512 (5), provides an alternate route of emergence of β-lactam resistance. In this mutant, Ldt$_{fm}$ is sufficient for peptidoglycan cross-linking because the chromosome of *E. faecium* harbors a single LD-transpeptidase gene, and 100% of the cross-links are generated by LD-transpeptidation in medium containing high concentrations of ampicillin (4). However, the classical DD-transpeptidation pathway remains functional, and, consequently, the selective pressure of imipenem applies on transpeptidases of DD and LD specificity. In our selection procedure (Fig. 6), modifications of the DD-transpeptidation pathway were selected by imipenem alone because mutants S1–S4 remained susceptible to the combination of ampicillin and imipenem. For this reason, we used ampicillin and imipenem to inactivate the DD-transpeptidases and select mutations specifically affecting the LD-transpeptidation pathway. Seven additional selection steps were required to obtain mutant S11, which was moderately resistant to imipenem. Only two of the seven steps led to substitutions in Ldt$_{fm}$, indicating that modifications of other unknown factors are involved in acquisition of resistance. For the DD-transpeptidases, emergence of β-lactam resistance also involves a combination of multiple modifications affecting non-penicillin-binding protein factors, several residues of a given penicillin-binding protein, and sometimes several penicillin-binding proteins (11–16). The requirement for multiple mutations accounts for the relative robustness of β-lactams with respect to the emergence of resistance by target modification. Our study extends this observation to Ldt$_{fm}$, indicating that LD-transpeptidases are attractive targets for drug development.

In order to investigate the kinetics of inactivation of Ldt$_{fm}$, we first showed that acylation of the active-site cysteine residue was irreversible (Fig. 2). Acylation of Ldt$_{fm}$ from the imipenem-resistant mutant S11 was also irreversible (supplemental Fig. S4). Strikingly, the acylenzyme appeared more stable than the drug because hydrolysis was only detected for the free drug in solution (Fig. 2 and supplemental Fig. S4). This is most probably a critical asset for antibacterial activity because *de novo* protein synthesis is the only source of active enzyme following acylation of Ldt$_{fm}$.

Demonstration of the irreversible nature of Ldt$_{fm}$ inactivation has greatly simplified the current analyses because reaction scheme 2 could be applied (Fig. 1). The same reaction scheme is used for DD-transpeptidases that display a negligible deacylation rate, generally under the assumption that the non-covalent complex *E*I, free enzyme, and free inhibitor are in rapid equilibrium (11, 17). Consequently, the kinetics of acylation based on spectrophotometric determination of β-lactam ring opening are classically analyzed by determining the dissociation constant K_D (k_{-1}/k_1) and the acylation rate k_{inact} or the ratio k_{inact}/K_D because saturation of the enzyme is often experimentally inaccessible. In our study, we have developed a radically different approach because imipenem and Ldt$_{fm}$ were not found to be in rapid equilibrium. Instead of simultaneously determining k_{inact} and K_D from the same kinetics at various inhibitor concentrations, we independently determined k_{inact} and k_1 based on absorbance and fluorescence kinetics, respectively. Briefly, k_{inact} was determined by the classical approach based on the relation between k_{obs} and inhibitor concentration (Fig. 3). The catalytic constant k_1 could be determined by spectrofluorimetry because formation of the non-covalent complex (*E*I) and of the acylenzyme (*E*I*) led to dramatically different intensities of fluorescence quenching (Fig. 4). This allowed us to monitor the three forms of the enzyme, whereas classical analyses of the DD-transpeptidases are based on determination of only the acylenzyme.

The kinetics of acylation of Ldt$_{fm}$ by imipenem revealed several features relevant to the *in vivo* activity of the drug. Because k_{inact} (4.5 min^{-1}) was much greater than k_{-1} (< 0.1 min^{-1}), the fate of the *E*I complex is almost exclusively to proceed into the irreversible acylation step. At the minimal drug concentration required to inhibit growth of mutant M512 (0.5 μg/ml or 1.7 μM), the pseudo-first-order constant k_1[I] (0.11 min^{-1}) is ~40-fold smaller than k_{inact} (4.5 min^{-1}). At this drug concentration, which is relevant to the *in vivo* situation, formation of the non-covalent complex is the limiting step. In contrast, the rates of acylation of Ldt$_{fm}$ (k_{inact}) and of formation of the complex (k_1) were both limiting at the higher drug concentrations used for *in vitro* determination of the catalytic constants (*e.g.* k_1[I] = 6.5 min^{-1} for an imipenem concentration of 100 μM). The rate of formation of the acylenzyme (k_1) appears low because a simulation indicated that 28 min were required for a 95% decrease in active enzyme (*E*) at an initial drug concentration of 0.5 μg/ml, corresponding to the MIC for mutant M512 (supplemental Fig. S5). This rate was, however, sufficient for efficient enzyme inhibition at the time scale of one generation (~90 min for mutant M512) because the non-covalent complex (*E*I) is committed to acylation, and formation of the acylenzyme (*E*I*) is irreversible. Thus, an imipenem concentration of 0.5 μg/ml was sufficient to inhibit Ldt$_{fm}$ and prevent the bacterium from escaping the

lethal effect of the drug by *de novo* synthesis of the target despite the modest values of k_1 and k_{inact}.

A decrease in the efficiency of enzyme acylation was expected to result in increased resistance to imipenem, and this possibility was explored by selecting mutant S11 and analyzing the impact of substitutions S405N and G430S on the kinetics of Ldt$_{fm}$ inactivation (Fig. 7). In combination, both substitutions led to a dramatic decrease in the rate of formation of the non-covalent complex because k_1 was reduced 68-fold (from 0.065 to 0.00095 μM^{-1} min^{-1}). Other catalytic constants of Ldt$_{fm}$ were not altered. As discussed previously, the substitutions did not expose the acylenzyme to hydrolysis (supplemental Fig. S4). Likewise, the value of k_{inact} was only slightly reduced (from 4.5 to 4.0 min^{-1}), indicating that reduced efficiency of Ldt$_{fm}$ acylation marginally contributed to the emergence of resistance. Strikingly, the 68-fold reduction in k_1 was commensurate to the increase in the MICs (32-fold). This is expected because the velocity of formation of the non-covalent complex ($d[EI]/dt = k_1[E][I]$) remains constant for inversely proportional variations of k_1 and imipenem concentration.

Simulations were performed to compare the impact of reductions in k_{inact} or k_1 on the level of resistance to imipenem (supplemental Fig. S5). A 68-fold decrease in k_{inact} (from 4.5 to 0.066 min^{-1}), while retaining the same value of k_1 (0.065 μM^{-1} min^{-1}), would result in a 95% decrease in the concentration of the active form of the enzyme (E) in 1.05 min at an imipenem concentration of 53 μM, corresponding to the MIC for mutant S11. The gain obtained by the 68-fold reduction in k_{inact} is only marginal because 0.89 min is required for inhibition of wild-type Ldt$_{fm}$ to the same extent. In contrast, the 95% threshold is reached in 60 min if the 68-fold decrease is applied to k_1 instead of k_{inact}. These simulations indicate that a decrease in the acylation rate may not be sufficient to achieve resistance because neither EI nor EI* is an active form of the enzyme, and an LD-transpeptidase with a low acylation rate is expected to be saturated by the drug. Thus, the analysis of the catalytic properties of Ldt$_{fm}$ indicates that a reduction in the rate of formation of the non-covalent complex should be a privileged route for *in vivo* acquisition of resistance because this proved to be the case for mutant S11.

In conclusion, we report for the first time the kinetic analyses of inactivation of a novel target of β-lactam antibiotics, which is unrelated to the classical DD-transpeptidases. We also report an original approach for separate evaluations of the rate constants of a two-step reaction involving non-covalent antibiotic binding prior to acylation of the catalytic nucleophile. By exploring the role of amino acid substitutions in Ldt$_{fm}$ in the emergence of carbapenem resistance, we have shown that this approach provides meaningful correlations between antibacterial activity and interaction of the drug with the target *in vitro*. This approach could therefore also be applied to the determination of structure-activity relationships in the development of new antibacterial agents targeting the LD-transpeptidases, in particular the enzymes from extensively resistant clinical isolates of *M. tuberculosis*. The irreversibility of acylation of Ldt$_{fm}$ by imipenem and the multiple steps required for *in vivo* emergence of resistance in our *E. faecium* model underscores the interest of LD-transpeptidases as drug targets.

Acknowledgment—We thank J. van Heijenoort for critical reading of the manuscript.

REFERENCES

1. Sauvage, E., Kerff, F., Terrak, M., Ayala, J. A., and Charlier, P. (2008) *FEMS Microbiol. Rev.* **32,** 234–258
2. Mainardi, J. L., Villet, R., Bugg, T. D., Mayer, C., and Arthur, M. (2008) *FEMS Microbiol. Rev.* **32,** 386–408
3. Mainardi, J. L., Fourgeaud, M., Hugonnet, J. E., Dubost, L., Brouard, J. P., Ouazzani, J., Rice, L. B., Gutmann, L., and Arthur, M. (2005) *J. Biol. Chem.* **280,** 38146–38152
4. Mainardi, J. L., Hugonnet, J. E., Rusconi, F., Fourgeaud, M., Dubost, L., Moumi, A. N., Delfosse, V., Mayer, C., Gutmann, L., Rice, L. B., and Arthur, M. (2007) *J. Biol. Chem.* **282,** 30414–30422
5. Mainardi, J. L., Legrand, R., Arthur, M., Schoot, B., van Heijenoort, J., and Gutmann, L. (2000) *J. Biol. Chem.* **275,** 16490–16496
6. Lavollay, M., Arthur, M., Fourgeaud, M., Dubost, L., Marie, A., Veziris, N., Blanot, D., Gutmann, L., and Mainardi, J. L. (2008) *J. Bacteriol.* **190,** 4360–4366
7. Hugonnet, J. E., Tremblay, L. W., Boshoff, H. I., Barry, C. E., 3rd, and Blanchard, J. S. (2009) *Science* **323,** 1215–1218
8. Hugonnet, J. E., and Blanchard, J. S. (2007) *Biochemistry* **46,** 11998–12004
9. Gupta, R., Lavollay, M., Mainardi, J. L., Arthur, M., Bishai, W. R., and Lamichhane, G. (2010) *Nat. Med.* **16,** 466–469
10. Biarrotte-Sorin, S., Hugonnet, J. E., Delfosse, V., Mainardi, J. L., Gutmann, L., Arthur, M., and Mayer, C. (2006) *J. Mol. Biol.* **359,** 533–538
11. Zapun, A., Contreras-Martel, C., and Vernet, T. (2008) *FEMS Microbiol. Rev.* **32,** 361–385
12. Rice, L. B., Bellais, S., Carias, L. L., Hutton-Thomas, R., Bonomo, R. A., Caspers, P., Page, M. G., and Gutmann, L. (2004) *Antimicrob. Agents Chemother.* **48,** 3028–3032
13. Sifaoui, F., Arthur, M., Rice, L., and Gutmann, L. (2001) *Antimicrob. Agents Chemother.* **45,** 2594–2597
14. Job, V., Carapito, R., Vernet, T., Dessen, A., and Zapun, A. (2008) *J. Biol. Chem.* **283,** 4886–4894
15. Chesnel, L., Carapito, R., Croizé, J., Dideberg, O., Vernet, T., and Zapun, A. (2005) *Antimicrob. Agents Chemother.* **49,** 2895–2902
16. Halfmann, A., Kovács, M., Hakenbeck, R., and Brückner, R. (2007) *Mol. Microbiol.* **66,** 110–126
17. Frère, J. M., Ghuysen, J. M., and Iwatsubo, M. (1975) *Eur. J. Biochem.* **57,** 343–351